

1 **Vertical partitioning of phosphate uptake among picoplankton groups in the low-P**

2 **Mediterranean Sea**

3

4

5 A. Talarmin^{1,4}, F. Van Wambeke¹, P. Lebaron^{2,3}, T. Moutin¹

¹ Aix-Marseille Univ., Mediterranean Institute of Oceanography (MIO), 13288, Marseille, Cedex 09, France; Université du Sud Toulon-Var, MIO, 83957, La Garde cedex, France; CNRS/INSU, MIO UMR 7294; IRD, MIO UMR235

² Sorbonne Universités, UPMC Univ. Paris 06, USR 3579, LBBM, Observatoire Océanologique, 66650, Banyuls/mer, France

³ CNRS, USR 3579, LBBM, Observatoire Océanologique, 66650 Banyuls/mer, France

⁴ present address Red Sea Research Center, 4700 King Abdullah University of Science and Technology, Thuwal, 23955-6900, Kingdom of Saudi Arabia

6 Corresponding Author: Agathe Talarmin (agathe.talarmin@gmail.com)

7

1 **Acknowledgments**

2

3 The authors would like to thank the captain and crew of the R/V L'Atalante, Veronique Cornet
4 for the nanomolar SRP data, Laetitia Bariat and Philippe Catala for providing part of the
5 phytoplankton and bacterial counts, respectively, Anna Lagaria, Stella Psarra and Josephine Ras
6 for Chl-a data, Romain Mauriac for the joined effort on turnover time measurements and all the
7 scientists who participated in the BOUM cruise. We acknowledge the crucial contribution of
8 Claude Courties who sorted all the samples on board. Finally, we address our gratitude to the 3
9 anonymous reviewers who allowed us to greatly improve this manuscript and underpinned
10 elements that needed clarification and further detailing.

11 This work is a contribution of the BOUM project (Biogeochemistry from the Oligotrophic to
12 Ultraoligotrophic Mediterranean, <http://www.com.univ-mrs.fr/BOUM>). It was funded by the
13 French national CNRS-INSU (LEFE-CYBER) program and the European IP SESAME
14 (Southern European Seas: Assessing and Modelling Ecosystem Changes), EC Contract No.
15 GOCE-036949. We acknowledge the French Research and Education Council for the funding of
16 A.T.'s Ph.D. training.

17

18

1 **Abstract**

2 Microbial transformations are key processes in marine phosphorus cycling. In this study, we
3 investigated the contribution of phototrophic and heterotrophic groups to Pi uptake fluxes in the
4 euphotic zone of the low-phosphate (Pi) Mediterranean Sea and estimated Pi uptake kinetic
5 characteristics. Surface SRP concentrations ranged $6 - 80 \text{ nmol L}^{-1}$ across the transect, and the
6 community Pi turnover times, assessed using radiolabeled orthophosphate incubations, were
7 longer in the western basin, where the highest bulk and cellular rates were measured. Using live
8 cell sorting, 4 vertical profiles of Pi uptake rates were established for heterotrophic prokaryotes
9 (Hprok), phototrophic picoeukaryotes (Pic) and *Prochlorococcus* (Proc), *Synechococcus* (Syn)
10 cyanobacteria. Hprok cells contributed to up to 82 % of total Pi uptake fluxes in the superficial
11 euphotic zone, through constantly high abundances ($2.7 - 10.2 \times 10^5 \text{ cells mL}^{-1}$) but variable
12 cellular rates ($6.6 \pm 9.3 \text{ amol P cell}^{-1} \text{ h}^{-1}$). Cyanobacteria achieved most of the Pi uptake (up to 62
13 %) around the deep chlorophyll maximum depth, through high abundances (up to $1.4 \times 10^5 \text{ Proc}$
14 cells mL^{-1}) and high cellular uptake rates (up to 40 and 402 amol P $\text{cell}^{-1} \text{ h}^{-1}$, respectively for
15 Proc and Syn cells). At saturating concentrations, maximum cellular rates up to 132 amol P cell^{-1}
16 h^{-1} were measured for Syn at St. C, which was 5 and 60 times higher than Proc and Hprok,
17 respectively. Pi uptake capabilities of the different groups likely contribute to their vertical
18 distribution in the low-Pi Mediterranean Sea, possibly along with other energy limitations.

19

1 **1. Introduction**

2 Understanding nutrient uptake strategies in microorganisms is a necessity to predict their
3 biogeochemical response to environmental changes. Heterotrophic (Hprok) and phototrophic
4 prokaryotes (cyanobacteria) dominate the planktonic biomass in oligotrophic areas of the surface
5 ocean and account for most of the carbon fluxes through the microbial loop (*Azam et al.*, 1983).
6 Nanomolar concentrations of orthophosphate (Pi) and Pi turnover times as low as minutes or
7 hours are seasonally observed in the Sargasso and the Mediterranean (e.g. *McLaughlin et al.*,
8 2013; *Moutin et al.*, 2002; *Sebastián et al.*, 2012; *Thingstad et al.*, 1998; *Wu et al.*, 2000). Pi is
9 the preferred form of phosphorus for most osmotrophs, but recent studies show that dissolved
10 organic phosphorus (DOP) can be a significant source of P as well, particularly in its most labile
11 forms like ATP (e.g. *Björkman and Karl*, 1994; *Björkman et al.*, 2012; *Casey et al.*, 2009;
12 *Duhamel et al.*, 2012; *Fu et al.*, 2006; *M.W. Lomas et al.*, 2010; *Sebastián et al.*, 2012). It is now
13 well established that concentrations of Pi in the environment impact uptake processes by
14 microbes, who rely on high affinity systems via active transport at low concentrations and high
15 capacity systems and diffusion at higher environmental Pi (e.g. *Knauss and Porter*, 1954;
16 *Nyholm*, 1977). Along with an increased stratification and oligotrophication of the surface ocean,
17 a widely spread size-shift in the structure of phytoplankton communities is expected, from nano-
18 and micro- eukaryotes to pico-sized cells, as observed in the North Pacific Subtropical Gyre
19 (*Church et al.*, 2002; *Karl et al.*, 2001). How phytoplankton and bacteria share P resources when
20 they are poorly available has been debated for over 30 years. The existence of different Pi
21 acquisition systems in microorganisms was highlighted in studies where Hprok systems were
22 found to be saturating at much lower Pi concentrations than phytoeukaryotes (> 3 μm : *Currie*
23 and *Kalf*, 1984; *Currie et al.*, 1986). Some eukaryotes possess mixotrophic capabilities and

1 grazing on P-richer prokaryotes can fill most of their requirements in P (*Christaki et al.*, 1999;
2 *Hartmann et al.*, 2011) as well as DOP hydrolysis induced by ectoenzymes (ATPases, alkaline
3 phosphatases, e.g.: *Webb*, 1992). Eukaryotic phytoplankton may compensate their low affinity
4 for the substrate at low concentrations (high Km) with high Pi storage capacity (*Cotner and*
5 *Biddanda*, 2002) compared to prokaryotes and a more efficient growth mechanism, i.e. a low
6 half-saturation constant for growth (Ks, *Rhee*, 1973). Pi uptake by microbes in natural
7 environments has largely been assessed using size fractionation. Studies concur on the high
8 contribution of the small size fractions (<0.8, <1, <2 or <3 µm) to Pi uptake fluxes (*Björkman*
9 and *Karl*, 1994; *Currie et al.*, 1986; *Moutin et al.*, 2002; *Tanaka et al.*, 2003; *Thingstad et al.*,
10 1993; *Thingstad et al.*, 1998). This contribution generally increases in aquatic systems with short
11 Pi turnover times and also in low-Pi systems after P amendments, emphasizing the idea that
12 heterotrophic prokaryotes are high competitors in P-deficient areas (e.g.: *Björkman et al.*, 2012;
13 *Currie et al.*, 1986; *Drakare*, 2002; *Labry et al.*, 2002). However, size fractionation offers a
14 limited resolution of microbial processes, especially in oligotrophic environments where
15 osmotrophs are small and where taxonomic and functional types overlap in size. The
16 development of combined radiolabeling techniques and cell sorting by flow cytometry has
17 improved the level of resolution to study Pi uptake strategies in heterotrophic and phototrophic
18 microbes (e.g.: *Björkman et al.*, 2012; *Casey et al.*, 2009; *Duhamel et al.*, 2012; *Michael W.*
19 *Lomas et al.*, 2014; *Talarmin et al.*, 2011b; *Zubkov et al.*, 2007)
20 When looking into the contribution of picoplanktonic groups to total Pi uptake, prokaryotes are
21 better competitors than eukaryotes. Among prokaryotes, measured cellular uptake rates of Pi
22 were higher for Syn compared to Hprok and Proc in the Sargasso Sea (*Michelou et al.*, 2011),
23 and higher for Proc compared to Hprok in the North Pacific Subtropical Gyre (*Björkman et al.*,

1 2012), especially during light incubation (*Duhamel et al.*, 2012). Nevertheless, the comparison
2 among those studies is not always possible, due to methodological differences (fixation, inducing
3 Pi leakage) or to different targeted groups. Finally, only one study suggests the adaptation of
4 microorganisms to P amendments (*Björkman et al.*, 2012), with concentration kinetics
5 experiments providing useful insights into their coexistence in low-Pi environments.
6 The present study investigates the contribution of sorted picoplankton groups to total Pi uptake
7 flux in the Pi-depleted stratified upper water column of the Mediterranean Sea (down to 200 m).
8 An estimation of kinetic constants (maximum Pi uptake rate- V^{max} , and the sum of the half-
9 saturation constant plus Pi natural concentration $K+S_n$) of $^{33}P_i$ -radiolabeled orthophosphate
10 uptake in sorted Hprok, cyanobacterial and picophytoplanktonic cells is also provided to
11 compare competitive abilities of the groups at different depths and under different ambient Pi
12 concentrations. In spite of the amount of phosphorus-related studies conducted in the
13 Mediterranean Sea, such experiments have never been carried out in this system. Our results
14 contribute to further understand how prokaryotic autotrophs and heterotrophs share scarce
15 resources when the phytoplankton biomass is dominated by prokaryotes.

16 **2. Material and Methods**

17 **2.1. Study sites and collection**

18 An east-west transect across the Mediterranean Sea was realized during the BOUM cruise
19 (Biogeochemistry from Oligotrophic to Ultraoligotrophic Mediterranean) on the French R/V
20 L'Atalante from 16 June to 20 July 2008 (Fig. 1). Samples were collected using 12-L Niskin
21 bottles mounted on a rosette equipped with a conductivity-temperature-density (CTD) profiler
22 and sensors for pressure, oxygen, photosynthetically available radiation (PAR), and chlorophyll

1 fluorescence. Pi uptake and turnover time measurements reported in this study were fully
2 processed onboard. Total chlorophyll-a (TChl-a) concentrations were determined as described in
3 (Crombet *et al.*, 2011). Critical depths and integrated nutrient concentrations were calculated as
4 described in (Moutin and Prieur, 2012). Pi turnover times were measured at each of the 30
5 stations at fixed depths of 5, 25, 50, 75, 100 and 125m. Vertical Pi uptake profiles of Pi uptake in
6 sorted groups at stations 9, 21, A and 25 are presented here, as well as concentration bioassay
7 experiments conducted at stations C, and A.

8 **2.2.Enumeration of phototrophs and heterotrophs using flow cytometry**

9 Triplicated aliquots of 1.8 ml were sampled and fixed with a 2 % (w/v) formaldehyde solution,
10 stored for at least 30 min at room temperature, flash frozen in liquid nitrogen and then stored at
11 –80°C until further processing onshore within 6 months. Samples were thawed an hour before
12 analysis and 1 µm yellow-green beads (Fluoresbrite, Polysciences) were systematically added as
13 a standard. The sheath fluid was filtered (< 0.2 µm) seawater and analyses were conducted with
14 the software Cell Quest Pro. Microbes were enumerated using a FACScan flow cytometer (BD
15 Biosciences) equipped with an air-cool argon laser (488 nm, 15 mW). The red fluorescence
16 signal of the chlorophyll *a* was collected on a long-pass filter (> 650 nm) to identify
17 phytoplankton groups including *Prochlorococcus* and pico-phytoeukaryotes, according to Marie
18 et al. (2000). *Synechococcus* cells were discriminated from other phototrophs using their orange
19 fluorescence signal (585/21 nm).

20 Samples for the enumeration of heterotrophic prokaryotes were stained with SYBRGreen I
21 (Invitrogen–Molecular Probes) at 0.025 % (vol/vol) final concentration for 15 min at room
22 temperature in the dark. Counts were performed using a FACSCalibur flow cytometer (BD

1 Biosciences) equipped with an air-cooled argon laser (488 nm, 15 mW). Stained bacterial cells,
2 were discriminated and enumerated according to their right-angle light scatter (SSC) and green
3 fluorescence of the nucleic acid dye (530/30 nm). Autotrophic prokaryotes were discarded from
4 this analysis based on their red fluorescence.

5 **2.3. Sample preparation for Pi uptake measurements**

6 Clean 30-mL polycarbonate Nalgene bottles were filled with 10 mL of seawater samples.
7 Preliminary measurements were conducted at the beginning of the cruise to adjust the incubation
8 conditions so that Pi uptake was linear with time. The methodology and calculations employed
9 for bulk and cell-normalized, group-specific Pi uptake rates were based on the protocol by
10 (*Talarmin et al.*, 2011b). Briefly, a radioactive working solution was freshly prepared on board
11 by diluting a carrier-free [^{33}P]-H₃PO₄ mother solution (Perkin Elmer, USA, 569.5×10^{12} Bq
12 mmol⁻¹) in 0.2 µm-filtered milliQ water, and added to the samples. ^{33}Pi incorporation at room
13 temperature, under natural light condition, was stopped by adding an excess amount (0.1 mM
14 final concentration) of a cold Pi solution. Samples were split in 3 aliquots of 5 mL (for bulk-
15 whole water- Pi uptake measurements), 3.5 mL (for sorting of phototrophic groups) and 1.5 mL
16 (for sorting of Hprok cells), and kept in the dark at 4 °C until further processing (<1 hour for the
17 5 ml subsamples, 10 minutes to 6 hours for the others). A cold Pi solution was added to blank
18 samples (final concentration of 0.1 mmol L⁻¹) 15 minutes prior to radiolabeling and processed
19 like other samples. Blank values represented on average 5.0 to below 13 % of regular values
20 estimated for bulk (n=11) and sorted groups (n=36), respectively. Blank values were
21 systematically subtracted from the counts, in dpm cell⁻¹, for the sorted samples. The radioactivity
22 was counted onboard within 5 hours after addition of the scintillation cocktail using a Packard
23 LS 1600 liquid scintillation counter.

1 **2.3.1. *In situ* Pi uptake rates**

2 At stations A, 9, 21 and 25, samples were collected at several depths in order to assess the
3 vertical distribution of the group-specific P_i uptake under ambient concentrations of P_i . Samples
4 were spiked with a final concentration of 20 pmol L⁻¹ of the ³³P-orthophosphate working solution
5 and incubated for 15 minutes.

6 **2.3.2. Concentration kinetics of Pi uptake**

7 Surface experiments carried out between stations B and C led to unsatisfying results where
8 signals were too weak for Pic and unstained Proc cells could not be detected. The upper deep
9 chlorophyll maximum (DCM) depth was then chosen as a biogeochemically consistent level,
10 considering that the depth of the DCM and nutriclines was expected to vary considerably along
11 the transect. Concentration kinetics experiments were conducted at stations 5, A, B and C by
12 adding increasing quantities of a cold KH₂PO₄ solution (0, 4, 8, 10, 15, 20, 40, 60, 80, 100 nmol
13 L⁻¹ added concentration, Sa). Samples were spiked with the radioactive working solution 15
14 minutes later, with an activity of 0.34 MBq per sample, i.e. a final radioactive P_i concentration of
15 60 pmol L⁻¹, and incubated for 45 minutes. Bulk P_i uptake rates, bulk P_i turnover times, bulk and
16 taxon-specific kinetic constants V^{max} (maximum velocity of P_i uptake) and $K+S_n$ (K being the
17 half-saturation constant and S_n the natural P_i concentration, their sum being determined as the
18 intersection of the plotted line with the x axis), were based on the work by *Thingstad et al.*
19 (1993). Such estimations were obtained using the linear regression of P_i turnover time versus Sa.

20 **2.3.3. Bulk Pi uptake measurements**

21 The 5-mL aliquots were gently filtered on a 0.2 µm polycarbonate membrane superimposing a
22 GF/D filter soaked with a cold Pi solution without rinsing. A 5-second increase of the vacuum

1 pressure ended the filtration to remove non-incorporated Pi. Filters were then placed in
2 scintillation vials with 5 mL of Phase Combining System scintillation cocktail (PCS, GE
3 Healthcare).

4 **2.3.4. Flow sorting of labeled picoplankton groups**

5 Other aliquots were processed by flow sorting on an onboard FACS Aria cell sorter (BD
6 Biosciences) equipped with two lasers: a 488 nm (13 mW, Coherent, Sapphire Solid State) and a
7 633 nm (11 mW, JDS Uniphase air-cooled HeNe), using the same detection strategy as for
8 enumeration of phototrophic and heterotrophic cells. The sheath fluid was 0.2- μ m filtered
9 seawater. The instrument was controlled by a computer equipped with the FACSDiva software
10 set on the four-way sorting 0/32/0 purity mode. Re-sorting of sorted samples was conducted
11 randomly to check for the purity of the sorts, which reached 98 %. Sorted cells were collected in
12 2-mL microcentrifuge tubes where PCS scintillation cocktail was added up to a final volume of 2
13 mL.

14 Experiments were replicated on one occasion, and cellular Pi uptake rates varied by less than 4%
15 in prokaryotic sorts and by 11% in Pic (n=4). Analytical error associated with cellular uptake
16 rates was about 10% and error on cell abundances around 5%.

17 **2.4. Soluble reactive phosphorus (SRP)**

18 SRP was measured at the nanomolar level according to the Rimmelin and Moutin procedure
19 (*Rimmelin and Moutin, 2005*), derived from the initial MAGIC method proposed by *Karl and*
20 *Tien* (1992), using 250-mL triplicates per depth. The detection limit of this technique was around
21 5 nmol L⁻¹.

1 **2.5. Statistical analyses and data treatment**

2 Averaged values are reported as mean \pm one standard deviation (sd). The Michaelis-Menten
3 equation was used with estimated V^{max} and $K+Sn$ to fit a Monod curve to the Pi uptake rates
4 measured. They were only shown when a significant between the model and the data correlation
5 was found ($p < 0.05$). Using the turnover time approach to determine kinetic parameters, V^{max}
6 and $K+Sn$ can always be determined, but only V^{max} is relevant in samples where $V=V^{max}$.

7 Biomass estimations were used to discuss our results, using our cell abundances and cellular P
8 quotas by *Bertilsson et al.* (2003) and *Ho et al.* (2003).

9 **3. Results**

10 **3.1. Environmental and biological conditions**

11 A westward shoaling of the DCM (Table 1) and nutricline depths (120 to 50 m and 200 to 50 m,
12 respectively) was observed along the transect. Total chlorophyll-a concentrations integrated over
13 150 meters were up to twice as high in the western basin (e.g. St. 25) compared to the Levantine
14 basin (e.g. St. 9; Table 1), emphasizing the strong oligotrophic state of the eastern waters.

15 SRP concentrations ranged 6 – 80 nmol L⁻¹, varying with depth and location (Table 1). The
16 highest maximum surface values were measured in the Western Basin (St. 21 and 25), possibly
17 due to incomplete stratification of the water column and the proximity to the Rhone River
18 compared to other stations. However, short Pi turnover times (0.8 to 10 h) were estimated (Fig.
19 2), revealing a high turnover of Pi in microbial communities along the whole transect at surface
20 depths. It is important to point out that the detection limit for SRP measurements was close to the
21 ambient concentrations, hence a potential overestimation of the latter and of Pi uptake rates

1 calculated using Sn. This caveat would not affect the main results about the relative capabilities
2 of sorted groups in a given sample to take up Pi, as the same Pi concentration was multiplied by
3 the turnover rates (h^{-1}) of each sorted group or bulk community for a given depth.

4 **3.2. Enumeration of microbial groups**

5 Hprok cells were the most abundant group, and varied little over sampled stations and depths,
6 with an average of $3.9 \pm 0.3 \times 10^5$ cells mL^{-1} (n=24), and ranging $2.7 \times 10^5 - 10.2 \times 10^5$ cells mL^{-1}
7 (Fig. 3). Abundances of Proc cells varied between undetected levels to 1.4×10^5 cells mL^{-1} .
8 Their pigment signature was too weak to be detected in surface waters without staining, therefore
9 many experiments are missing data for Proc cells above 50 m. Syn cells were the most abundant
10 at the coastal station 25 (7.7×10^4 cells mL^{-1} at 40 m) and the least abundant in the deep euphotic
11 zone (130 m St. A, 0.6×10^3 cells mL^{-1} ; Fig. 3). Finally, Pic cells were the most abundant in the
12 Western Basin, ranging 230 cells mL^{-1} up to 0.3×10^5 cells mL^{-1} .

13 **3.3. Bulk Pi uptake**

14 Pi uptake rates ranged between 0.03 and 21.6 nmol P $\text{L}^{-1} \text{ h}^{-1}$ and varied by a factor of 10 along
15 the water column at stations with the lower turnover times (9 and 21), while rates could be
16 multiplied by 200 from one depth to the other at St. 25 and A (Fig. 4). No significant correlation
17 was found between Pi uptake rates and SRP concentrations. In the Western basin, SRP
18 concentrations were close to or no more than twice as high as in the Eastern basins (17.2 ± 14.0
19 nmol P $\text{L}^{-1} \text{ h}^{-1}$, n=15, across the sampled depths), but Pi turnover times however could be 300
20 higher in the Western basin.

21 **3.4. Group-specific Pi uptake**

1 When all available, summed contributions of the 4 sorted groups to Pi uptake under ambient Pi
2 concentrations represented $83.3 \pm 30\%$ of the bulk signal (n=8). At the 4 stations, a higher
3 contribution (up to 82.5% at St. A; Fig. 4) of Hprok cells was observed, with cellular uptake
4 rates between 0.74 and 27.75 amol P cell $^{-1}$ h $^{-1}$ (Table 1) between surface and 25 or 50 m. In the
5 vicinity of the DCM, cyanobacterial cells were the major contributors to bulk signal (up to 72%
6 at St. A; Fig. 4), mostly Proc cells in open sea samples (Fig. 3 a, c). Syn cells contributed to bulk
7 signal by 53 % at the coastal station, where they reached the highest abundance measured during
8 the cruise, while their average contribution over the cruise was of $16.3 \pm 14\%$ (n=18).

9 Differences between cellular mean rates were not significant ($p=0.06$), due to a high variability
10 across samples for a single group ($CV \geq 84\%$). However, in half of the samples for which both
11 Syn and Pic were sorted, cellular Pi uptake rates were higher in Syn than in Pic cells (Table 1).
12 The biomass of Pic in the bioassay of St. A reached 1.2 nmol P L $^{-1}$, and ranged 15.7 – 34.4 nmol
13 P L $^{-1}$ along the profile at St. 25, which was 300, and 25 – 55 higher than the biomass of Syn,
14 respectively. Proc estimated biomass was in the same order of magnitude as Syn, around 0.3
15 nmol P L $^{-1}$, and Hprok biomass was twice lower than Pic. In 22 out of 23 sorts, Hprok specific
16 rates were consistently lower compared to cyanobacteria. At station A, volumetric Pi uptake
17 rates were the highest for picoeukaryotes, and consistently high for all sorted groups (Table 1).
18 Over all experiments, cellular uptake rates ranged 2.6 – 402, 3.6 – 40.0, 8.4 – 134.8, and 0.05 –
19 36.1 amol P cell $^{-1}$ h $^{-1}$ for Syn, Proc, Pic, and Hprok, respectively (Table 1).

20 **3.5. Kinetics of the Pi uptake**

21 Data from St. C and A only could be used to explore kinetic characteristics, while no response to
22 Pi addition was observed at St. 5 and B. Cellular (V_c^{\max}) and volumetric (V^{\max}) rates are reported
23 in Table 2. Signals measured at St. B and C in sorted Pic cells during the isotope dilution

1 experiments did not show any dose response, and therefore no kinetic parameters were
2 estimated. At St. A and C, the highest V^{max} was obtained for cyanobacterial sorts (Table 2).
3 Cellular maximum uptake rates (V_c^{max}) were found in different relative order at both stations,
4 with V_c^{max} Syn > Proc > Hprok at St. C and Pic > Syn > Proc at St. A (Table 2). Estimations of
5 the K_{+S_n} constant Proc and Pic cells at St. A and Syn cells at St. C were comparable and about 5
6 times lower than the value measured for Syn cells at St. A (128.4 nmol P L⁻¹). At St. A, Syn,
7 Proc and Pic exhibited a subsaturated Pi uptake under natural conditions (rates measured from
8 profiles compared to V^{max} at this depth) with 13, 44 and 86 %, respectively. Both cellular and
9 volumetric maximum rates were drastically lower at St. A compared to St. C, while K_{+S_n} values
10 in the bulk and Syn sorts were higher at St. A.

11 **4. Discussion**

12 A recent review on phosphorus marine biogeochemistry pointed out marine microbial cycling of
13 phosphorus as the most dynamic and complex cycle of all (Karl, 2014). With consistently short
14 Pi turnover times (< 10 h) measured in surface samples from the eastern basin, congruent with
15 previous studies (Flaten *et al.*, 2005; Moutin *et al.*, 2002), our study emphasizes the short time
16 scale and dynamics of Pi cycling in the Mediterranean. Low Pi turnover times deepening towards
17 the East in the while SRP concentrations did not show a clear longitudinal and suggest a higher
18 limitation of microbial communities in the Eastern basin.

19 **4.1. Taxon-specific Pi uptake**

20 Cellular Pi uptake rates suggest that there was variability across sorted groups, with Hprok
21 having the lowest rates in most samples. When all 3 phototrophic groups were successfully
22 sorted, there was not a single group clearly showing higher cellular Pi uptake rates, like there

were in samples from the North Atlantic (e.g. Pic *Lomas et al.*, 2014, Syn in *Michelou et al.*, 2011 and Syn and Pic in *Zubkov et al.*, 2007). We measured cellular Pi uptake rates for Proc cells over 10 fold higher (16.1 ± 13.6 amol P cell $^{-1}$ h $^{-1}$, n=15) in the Mediterranean Sea compared to rates measured in the Sargasso Sea (< 1 amol P cell $^{-1}$ h $^{-1}$: *Casey et al.*, 2009; *Michelou et al.*, 2011; *Zubkov et al.*, 2007]). We suggest 4 main reasons to explain differences across regions: i) different composition of the cyanobacterial community between the Sargasso Sea and the Mediterranean, notably clade HL II which is underrepresented in the Mediterranean (*Mella-Flores et al.*, 2011) ii) the low proportion of Proc cells (<10%) able to utilize Pi in the subsurface layers of the Sargasso Sea (*Martínez et al.*, 2012), iii) different proportions of live versus dead cyanobacterial cells in the Sargasso and Mediterranean Sea (*Agusti*, 2004), and iv) measurements conducted on fixed samples in the mentioned studies from the Sargasso Sea, possibly involving a significant leakage of intracellular Pi (*Talarmin et al.*, 2011b). The dominance of Syn in Pi uptake fluxes above the DCM at St. 25 was likely due to their higher affinity for Pi compared to Pic cells, because their biomass was 50 times lower than Pic.

4.2. Kinetic parameters in sorted groups

Summed volumetric V $^{\max}$ of sorted groups added up to the community V $^{\max}$ or below. Non-sorted large protists may have higher maximum Pi uptake rates per cell (*Casey et al.*, 2009) or the ability to store large amounts of Pi in case of upwelled or deposited inputs. The kinetic experiment results presented here shall be interpreted very cautiously due to their scarcity, and they should serve as a starting point to infer Pi uptake strategies with regard to environmental conditions. At Station C, the groups expected to have a higher affinity for low concentration did not show a response to Pi additions because they were taking up Pi at the maximum velocity. *Synechococcus* was described as a group able to respond rapidly and significantly to pulsed Pi

1 events (*Moutin et al.*, 2002), which could be supported by the fact that Pi uptake under ambient
2 SRP concentrations was not saturated at St. A or St. C and that they did show a response to Pi
3 additions at both stations. Our data also suggest that microbial communities have the potential to
4 take up more Pi when Pi turnover times are short. Per cell Pi uptake rates converted in per
5 volume Pi uptake rates have shown opposite trends, with cyanobacteria harvesting Pi more
6 efficiently than larger phytoplankton (*Casey et al.*, 2009). With their high surface-to-volume
7 ratio (*Azam et al.*, 1983), prokaryotes with a biovolume below 40 μm^3 may not be submitted to
8 the theoretical surface-limited growth rate, due to a poor cellular machinery compared to the
9 absorbing capability (*Dao*, 2013), hence their higher cellular uptake rates under low
10 concentrations compared to picoeukaryotes.

11 **4.3. Contribution of the sorted groups to total Pi uptake**

12 Biogeochemically, using volumetric Pi uptake rates is more valuable than the cell-specific values
13 to highlight the overall contribution of one group to Pi fluxes through the marine microbial P
14 cycle. Down to about 25 m above the DCM, at the 4 stations sampled for depth profiles, the main
15 contributors to Pi uptake fluxes were the heterotrophic prokaryotes. *Michelou et al.* (2011) found
16 dominance of bulk Pi uptake by Hprok in the Sargasso Sea, in surface and DCM layers. These
17 authors determined that cyanobacteria (Proc + Syn) contributed to less than 10 % of the Pi
18 uptake fluxes. These contributions were a result of i) low Syn abundances, although this group
19 exhibited 2 to 5-fold higher taxon-specific uptake rates than Proc and Hprok and intermediate
20 Proc abundances, combined with ii) lower cell specific rates for Proc (0.4 amol P cell $^{-1}$ h $^{-1}$). In
21 contrast, we found in the Mediterranean Sea a higher contribution of cyanobacteria close to the
22 DCM compared to upper layers, mostly due to abundances higher than those observed in the
23 North Atlantic at the time of the cruise (*Michelou et al.*, 2011).

1 The companion paper of these experiments published earlier by Casey et al. (2009) found no
2 clear difference in the contribution of Proc and Syn to Pi utilization. Proc contributed to 45% of
3 the bulk Pi uptake in the North Atlantic (Zubkov *et al.*, 2007), which is within the range of our
4 measurements (<LD – 62.9%). In the North Pacific Subtropical Gyre, Pro and Hprok cells did
5 not reveal different contributions to total Pi uptake fluxes, despite taxon-specific rates 3-fold
6 higher for Proc than for Hprok (Björkman *et al.*, 2012). At the SOLA station of the eastern
7 Mediterranean Sea (Banyuls sur mer, France), Syn contributed the most to the total Pi uptake
8 (35%) among 3 sorted groups, while Pic and Hprok showed low and non-significantly different
9 contributions (Talarmin *et al.*, 2011b). For the first time, our results suggest that the uptake of Pi
10 at an offshore oligotrophic location was not dominated by a single group of microbes in the
11 upper euphotic zone. The present study together with a previously published survey conducted
12 during the same cruise on leucine incorporation in sorted groups (Talarmin *et al.*, 2011a) showed
13 the importance of *Prochlorococcus* cells in elemental fluxes in the Mediterranean Sea, as it was
14 previously demonstrated in the Sargasso Sea (Casey *et al.*, 2007).

15 The unexplained fraction in the contribution profiles could be attributed to missing sorts or
16 taxonomic groups that were not taken into account. For instance, viruses and bacterivorous
17 mixotrophic ciliates or nanoflagellates, which by-pass nutrients to the highest trophic levels of
18 the microbial loop by grazing (Krom *et al.*, 2005; Paffenhöfer *et al.*, 2007), or attached bacteria,
19 could also contribute to bulk P_i uptake fluxes. In freshwater systems, they could take up Pi and
20 amino acid at higher rates than free-living bacteria (Paerl and Merkel, 1982; Simon, 1985).
21 Finally, we also considered the possibility that Proc cells from surface layers had too low
22 chlorophyll a content to be discriminated from Hprok in stained samples, resulting in an

1 overestimation of the Hprok contribution to bulk Pi uptake in the surface samples where Proc
2 cells were not detected.

3 **4.4. Other limitations**

4 The vertical partitioning of Pi uptake observed in the present study suggested that different
5 nutrient uptake strategies and capabilities may contribute to explain the vertical structure of
6 microbial communities throughout the water column. In the surface where SRP concentrations
7 are the lowest, only organisms with the lowest K+Sn can utilize Pi efficiently, i.e. Proc and
8 Hprok cells. The cyanobacterial contribution to Pi uptake possibly decreased below the DCM
9 because of light limitation (*Duhamel et al.*, 2012). During this cruise, a mesocosm study showed
10 that surface communities were submitted to N and P co-limitation or N limitation, but no strict P-
11 limitation (*Tanaka et al.*, 2011), and no nutrient (N, P) limitation was found at St. A. Dust
12 deposition were found to be 89% from anthropogenic sources at this station (*Ternon et al.*,
13 2011), which may provide more or different P sources than in the more eastern basins isolated
14 from all inputs. A larger effort in measuring environmental data, combined to phylogenetic
15 analyses of the sorted groups would help to further link the diversity of microbes to their Pi
16 uptake performances. Such experiments have been conducted in mesocosm conditions and
17 showed that different bacterial taxa responded to Pi additions with different strategies in the
18 Mediterranean Sea (*Sebastián et al.*, 2012). The concept of competition among microbes for a
19 limited resource in natural environments is challenged by the numerous potential sources of
20 growth limitation and the high diversity of cytometric groups (e.g.: *Kashtan et al.*, 2014; *Marie*
21 *et al.*, 2010).

22

1 **Conclusion**

2 While a few taxon-specific Pi uptake rates from various areas were published in the past 7 years,
3 our study was the first focusing on the Mediterranean Sea and uncovering a vertical partition of
4 Pi uptake fluxes among microbial groups. Each group studied in this survey seemed to have a
5 key role in Pi cycling under given environmental conditions, whether it through high affinity for
6 Pi at low concentrations (Hprok and Proc), or the ability to take up Pi at high rates (Syn and Pic)
7 at some depths. The variability observed within and across sorted groups seems to reflect
8 different kinetic abilities ranging along a continuum of Pi uptake strategies as well as
9 phylogenetic diversity within cytometric groups.

10 We found that different groups were dominating bulk Pi uptake fluxes at different depths, with
11 Hprok contributing the most in the surface, subsurface layers and likely also the bottom layers of
12 the euphotic zone, while cyanobacteria were dominating fluxes around the DCM zone. Multiple
13 nutrient and energy limitations need to be further investigated to better understand this vertical
14 partition of Pi uptake in oligotrophic waters.

References

- Agusti, S. (2004), Viability and niche segregation of Prochlorococcus and Synechococcus cells across the Central Atlantic Ocean, *Aquat. Microb. Ecol.*, 36, 53-59.
- Azam, F., T. Fenchel, J. G. Field, J. S. Gray, L. A. Meyer-Reil, and F. Thingstad (1983), The Ecological Role of Water-Column Microbes in the Sea, *Marine Ecology Progress Series*, 10, 257-263.
- Bertilsson, S., O. Berglund, D. M. Karl, and S. W. Chisholm (2003), Elemental Composition of Marine Prochlorococcus and Synechococcus: implications for the Ecological Stoichiometry of the Sea, *Limnology and Oceanography*, 48(5), 1721-1731.
- Björkman, K., and D. M. Karl (1994), Bioavailability of inorganic and organic phosphorus compounds to natural assemblages of microorganisms in Hawaiian coastal waters, *Marine Ecology Progress Series*, 111, 265-273.
- Björkman, K., S. Duhamel, and D. M. Karl (2012), Microbial Group Specific Uptake Kinetics of Inorganic Phosphate and Adenosine-5'-Triphosphate (ATP) in the North Pacific Subtropical Gyre, *Frontiers in Microbiology*, 3.
- Casey, J. R., M. W. Lomas, J. Mandecki, and D. E. Walker (2007), *Prochlorococcus* contributes to new production in the Sargasso Sea deep chlorophyll maximum *Geophysical Research Letters*, 34.
- Casey, J. R., M. W. Lomas, V. K. Michelou, S. T. Dyhrman, E. D. Orchard, J. W. Ammerman, and J. B. Sylvan (2009), Phytoplankton taxon-specific orthophosphate (Pi) and ATP utilization in the western subtropical North Atlantic, *Aquatic Microbial Ecology*, 58(1), 31-44.
- Christaki, U., F. Van Wambeke, and J. R. Dolan (1999), Nanoflagellates (mixotrophs, heterotrophs and autotrophs) in the oligotrophic eastern Mediterranean: standing stocks, bacterivory and relationships with bacterial production, *Marine Ecology Progress Series*, 181, 297-307.
- Church, M. J., H. Ducklow, and D. M. Karl (2002), Multiyear increases in dissolved organic matter inventories at Station ALOHA in the North Pacific Subtropical Gyre, *Limnology & Oceanography*, 47(1), 1-10.
- Cotner, J. B., and B. A. Biddanda (2002), Small Players, Large Role: Microbial Influence on Biogeochemical Processes in Pelagic Aquatic Ecosystems, *Ecosystems*, 5(2), 105-121.
- Crombet, Y., K. Leblanc, B. Quéguigner, T. Moutin, P. Rimmelin, J. Ras, H. Claustre, N. Leblond, L. Oriol, and M. Pujo-Pay (2011), Deep silicon maxima in the stratified oligotrophic Mediterranean Sea, *Biogeosciences*, 8, 459-475.
- Currie, D. J., and J. Kalff (1984), A comparison of the abilities of freshwater algae and bacteria to acquire and retain phosphorus, *Limnology & Oceanography*, 29(2), 298-310.
- Currie, D. J., E. Bentzen, and J. Kalff (1986), Does algal-bacterial phosphorus partitioning vary among lakes? a comparative study of orthophosphate uptake and alkaline phosphatase activity in freshwater, *Can. J. Fish. Aquat. Sci.*, 43(2), 311-318.
- Dao, M. H. (2013), Reassessment of the cell surface area limitation to nutrient uptake in phytoplankton, *Marine Ecology Progress Series*, 489, 87-92.
- Drakare, S. (2002), Competition between Picoplanktonic Cyanobacteria and Heterotrophic Bacteria along Crossed Gradients of Glucose and Phosphate, *Microbial Ecology*, 44(4), 327-335.
- Duhamel, S., K. M. Björkman, and D. M. Karl (2012), Light dependence of phosphorus uptake by microorganisms in the subtropical North and South Pacific Ocean, *Aquatic Microbial Ecology*, 67(3), 225-238.
- Flaten, G. A. F., et al. (2005), Studies of the microbial P-cycle during a Lagrangian phosphate-addition experiment in the Eastern Mediterranean, *Deep Sea Research II*, 52, 2928-2943.

- Fu, F. X., Y. Zhang, Y. Feng, and D. A. Hutchins (2006), Phosphate and ATP uptake and growth kinetics in axenic cultures of the cyanobacterium *Synechococcus* CCMP 1334, *European Journal of Phycology*, 41, 15-28.
- Hartmann, M., C. Grob, D. J. Scanlan, A. P. Martin, P. H. Burkill, and M. V. Zubkov (2011), Comparison of phosphate uptake rates by the smallest plastidic and aplastidic protists in the North Atlantic subtropical gyre, *FEMS Microbiology Ecology*, 78(2), 327-335.
- Ho, T.-Y., A. Quigg, Z. V. Finkel, A. J. Milligan, K. Wyman, P. G. Falkowski, and F. M. M. Morel (2003), The elemental composition of some marine phytoplankton, *Journal of Phycology*, 39(6), 1145-1159.
- Karl, D. M. (2014), Microbially Mediated Transformations of Phosphorus in the Sea: New Views of an Old Cycle, *Annual Review of Marine Science*, 6(1), 279-337.
- Karl, D. M., and G. Tien (1992), MAGIC: A sensitive and precise method for measuring dissolved phosphorus in aquatic environments, *Limnol. Oceanogr.*, 37(1), 105-116.
- Karl, D. M., R. R. Bidigare, and R. M. Letelier (2001), Long-term changes in plankton community structure and productivity in the North Pacific Subtropical Gyre: The domain shift hypothesis, *Deep Sea Research Part II: Topical Studies in Oceanography*, 48(8-9), 1449-1470.
- Kashtan, N., et al. (2014), Single-cell genomics reveals hundreds of coexisting subpopulations in wild *Prochlorococcus*, *Science*, 344, 416-420.
- Knauss, H. J., and J. W. Porter (1954), The absorption of inorganic ions by Chlorella pyrenoidosa, *Plant physiology*, 29(3), 229-234.
- Krom, M. D., et al. (2005), Nutrient cycling in the south east Levantine basin of the eastern Mediterranean: Results from a phosphorus starved system, *Deep Sea Research Part II: Topical Studies in Oceanography*, 52(22-23), 2879-2896.
- Labry, C., A. Herblant, and D. Delmas (2002), The role of phosphorus on planktonic production of the Gironde plume waters in the Bay of Biscay, *Journal of Plankton Research*, 24(2), 97-117.
- Lomas, M. W., J. A. Bonachela, S. A. Levin, and A. C. Martiny (2014), Impact of ocean phytoplankton diversity on phosphate uptake, *Proceedings of the National Academy of Sciences*, 111(49), 17540-17545.
- Lomas, M. W., A. L. Burke, D. A. Lomas, D. B. Bell, C. Shen, S. T. Dyhrman, and J. W. Ammerman (2010), Sargasso Sea phosphorus biogeochemistry: an important role for dissolved organic phosphorus (DOP), *Biogeosciences*, 7, 695-710.
- Marie, D., X. L. Shi, F. Rigaut-Jalabert, and D. Vaultot (2010), Use of flow cytometric sorting to better assess the diversity of small photosynthetic eukaryotes in the English Channel, *FEMS Microbiology Ecology*, 72(2), 165-178.
- Martínez, A., M. S. Osburne, A. K. Sharma, E. F. DeLong, and S. W. Chisholm (2012), Phosphite utilization by the marine picocyanobacterium *Prochlorococcus* MIT9301, *Environmental Microbiology*, 14(6), 1363-1377.
- McLaughlin, K., J. A. Sohm, G. A. Cutter, M. W. Lomas, and A. Paytan (2013), Phosphorus cycling in the Sargasso Sea: Investigation using the oxygen isotopic composition of phosphate, enzyme-labeled fluorescence, and turnover times, *Global Biogeochem. Cycles*, 27(2), 375-387.
- Mella-Flores, D., et al. (2011), Is the distribution of *Prochlorococcus* and *Synechococcus* ecotypes in the Mediterranean Sea affected by global warming?, *Biogeosciences*, 8, 2785-2804.
- Michelou, V. K., M. W. Lomas, and D. L. Kirchman (2011), Phosphate and adenosine-5'-triphosphate uptake by cyanobacteria and heterotrophic bacteria in the Sargasso Sea, *Limnology & Oceanography*, 56(1), 323-332.
- Moutin, T., and L. Prieur (2012), Influence of anticyclonic eddies on the Biogeochemistry from the Oligotrophic to the Ultraoligotrophic Mediterranean (BOUM cruise), *Biogeosciences*, 9(10), 3827-3855.
- Moutin, T., T. F. Thingstad, F. Van Wambeke, D. Marie, G. Slawyk, P. Raimbault, and H. Claustre (2002), Does Competition for Nanomolar Phosphate Supply Explain the Predominance of the Cyanobacterium *Synechococcus*?, *Limnol. Oceanogr.*, 47, 1562-1567.

- Nyholm, N. (1977), Kinetics of phosphate limited algal growth, *Biotechnology and Bioengineering*, 19(4), 467-492.
- Paerl, H., and S. Merkel (1982), The effects of particles on phosphorus assimilation in attached vs. free floating microorganisms, *Arch. Hydrobiol.*, 93, 125-134.
- Paffenhöfer, G. A., B. F. Sherr, and E. B. Sherr (2007), From small scales to the big picture: persistence mechanisms of planktonic grazers in the oligotrophic ocean, *Marine Ecology*, 28(2), 243-253.
- Rhee, G. Y. (1973), A continuous culture study of phosphate uptake, growth rate and polyphosphate in *Scenedesmus* sp., *Journal of Phycology*, 9(4), 495-506.
- Rimmelin, P., and T. Moutin (2005), Re-examination of the MAGIC method to determine low orthophosphate concentration in seawater, *Analytica Chimica Acta*, 548(1-2), 174-182.
- Sebastián, M., P. Pitta, J. M. González, T. F. Thingstad, and J. M. Gasol (2012), Bacterioplankton groups involved in the uptake of phosphate and dissolved organic phosphorus in a mesocosm experiment with P-starved Mediterranean waters, *Environmental Microbiology*, 14(9), 2334-2347.
- Simon, M. (1985), Specific uptake rates of amino acids by attached and free-living bacteria in a mesotrophic lake, *Applied and Environmental Microbiology*, 49(5), 1254-1259.
- Talarmin, A., F. Van Wambeke, P. Catala, C. Courties, and P. Lebaron (2011a), Flow cytometric assessment of specific leucine incorporation in the open Mediterranean, *Biogeosciences*, 8, 253-265.
- Talarmin, A., F. Van Wambeke, S. Duhamel, P. Catala, T. Moutin, and P. Lebaron (2011b), Improved methodology to measure taxon-specific phosphate uptake in live and unfiltered samples, *Limnology & Oceanography: Methods*, 9, 443-453.
- Tanaka, T., F. Rassoulzadegan, and T. F. Thingstad (2003), Measurements of phosphate affinity constants and phosphorus release rates from the microbial food web in Villefranche Bay, northwestern Mediterranean, *Limnology & Oceanography*, 48(3), 1150-1160.
- Tanaka, T., et al. (2011), Lack of P-limitation of phytoplankton and heterotrophic prokaryotes in surface waters of three anticyclonic eddies in the stratified Mediterranean Sea, *Biogeosciences*, 8, 525-538.
- Ternon, E., C. Guieu, C. Ridame, S. L'Helguen, and P. Catala (2011), Longitudinal variability of the biogeochemical role of mediterranean aerosols, *Biogeosciences*, 8, 1067-1080.
- Thingstad, T. F., E. F. Skjoldal, and R. A. Bohne (1993), Phosphorus cycling and algal-bacterial competition in Sandsfjord, western Norway, *Marine Ecology Progress Series*, 99, 239-259.
- Thingstad, T. F., U. L. Zweifel, and F. Rassoulzadegan (1998), P limitation of heterotrophic bacteria and phytoplankton in the northwest Mediterranean, *Limnol. Oceanogr.*, 43(1), 88-94.
- Webb, M. R. (1992), A continuous spectrophotometric assay for inorganic phosphate and for measuring phosphate release kinetics in biological systems, *Proceedings of the National Academy of Sciences of the United States of America*, 89(11), 4884-4887.
- Wu, J., W. Sunda, E. A. Boyle, and D. M. Karl (2000), Phosphate Depletion in the Western North Atlantic Ocean, *Science*, 289(5480), 759-762.
- Zubkov, M. V., I. Mary, E. M. S. Woodward, P. E. Warwick, B. M. Fuchs, D. J. Scanlan, and P. H. Burkhill (2007), Microbial control of phosphate in the nutrient-depleted North Atlantic subtropical gyre, *Environmental Microbiology*, 9(8), 2079-2089.

Table 1. Environmental context of the experiments: sampled depth (m), depth of the deep chlorophyll maximum (DCMd), 0 – 150 m integrated chl *a* concentrations, SRP concentrations (mean ± sd), and cellular rates of Pi uptake measured in sorted groups *Synechococcus* (Syn), *Prochlorococcus* (Proc), picoeukaryotes (Pic) and heterotrophic prokaryotes (Hprok) measured under ambient concentrations. NA: data not available

Station	Depth (m)	DCMd (m)	Chl <i>a</i> int (mg C m ⁻²)	[SRP] (nM)	Cellular Pi uptake rate (amol P cell ⁻¹ h ⁻¹)			
					Syn	Proc	Pic	Hprok
C	100	108	25.10	12.8 ± 6.7	49.8	17.5	NA	1.2
9	5	128	16.20	20.2 ± 2.3	58.7	NA	NA	27.7
9	50			17.6 ± 1.6	14.0	NA	NA	0.7
9	75			12.4 ± 3.7	17.6	NA	NA	7.6
9	105			23.1 ± 3.7	41.7	35.5	NA	7.1
9	120			13.6 ± 1.4	46.5	39.9	NA	13.5
5	50	114	24.70	12.7 ± 6.7	43.0	13.0	NA	0.4
B	100	141	21.20	8.6 ± 0.5	24.3	20.3	NA	36.1
21	5	87	22.40	9.6 ± 1.9	401.6	NA	NA	3.6
21	50			13.1 ± 3.6	9.6	12.7	NA	2.6
21	70			14.4 ± 2.0	9.0	2.2	8.4	0.2
21	85			80.0 ± 17.6	23.5	5.8	49.4	0.7
A	6	88	24.70	10.6 ± 2.8	24.1	NA	8.6	11.5
A	13			5.8 ± 2.0	10.7	NA	4.0	5.8
A	25			6.3 ± 1.0	5.8	NA	3.3	3.2
A	75			8.3 ± 3.9	8.6	11.7	11.7	1.8
A	90			8.3 ± 0.8	13.1	9.5	33.7	0.4
A	100			16.4 ± 1.4	25.1	1.6	7.9	0.1
A	110			24.2 ± 3.4	5.0	1.5	7.3	NA
A	130			20.2 ± 1.3	5.7	3.6	3.8	0.1
25	5	51	38.50	17.3 ± 2.3	68.7	NA	44.9	8.7
25	25			18.00	48.7	37.2	55.5	16.2
25	40			18.00	NA	30.2	67.0	1.3
25	50			18.67	49.0	NA	134.8	0.8
25	60			19.10	NA	NA	NA	NA

Table 2. P_i uptake kinetic characteristics of the bulk community and sorted groups: V^{max} is the theoretical volumetric maximum uptake rate of a group, V_c^{max} is the cellular maximum uptake rate, and $K+S_n$ is the theoretical sum of the half saturation constant for uptake and the natural $[P_i]$. LD: below the limit of detection (< 3 blank values). NA: data not available

St.	z (m)	TPi (h)	V_c^{max} (amol P cell $^{-1}$ h $^{-1}$)				V^{max} (nmol P L $^{-1}$ h $^{-1}$)				$K+S_n$ (nmol P L $^{-1}$)					
			Syn	Proc	Pic	Hprok	Bulk	Syn	Proc	Pic	Hprok	Bulk	Syn	Proc		
C	100	3.9	132	21	LD	2	4.0	1.8	1.1	LD	0.6	15.3	22.9	NA	LD	NA
A	90	370.9	12	1	99	NA	0.2	0.03	0.02	0.02	NA	62.6	128.4	22.7	27.7	NA

Table S1. Detailed values of bulk Pi uptake rates and contribution of the groups to bulk Pi uptake at St. 9, St. 21, St. A and St. 25. NA= no available data

Station	Depth (m)	Bulk Pi uptake rate (nmol L ⁻¹ h ⁻¹)	Contribution to total Pi uptake (%)			
			Syn	Proc	Pic	Hprok
9	5	12.51	1.33	NA	NA	59.64
9	50	5.56	1.31	NA	NA	52.83
9	75	6.53	5.73	NA	NA	42.56
9	105	9.37	4.17	5.60	NA	48.54
9	120	1.22	14.02	51.62	NA	12.08
21	5	5.96	2.05	NA	NA	33.74
21	50	5.29	0.76	3.26	NA	34.42
21	70	0.91	7.11	8.26	0.44	9.85
21	85	1.79	2.77	3.64	1.45	21.72
A	6	6.64	2.40	NA	0.11	64.29
A	13	3.47	1.32	NA	0.10	74.71
A	25	1.94	0.63	NA	0.17	82.54
A	75	2.84	4.62	56.40	0.45	36.80
A	90	0.98	8.98	62.87	10.19	21.42
A	100	0.08	14.15	34.70	12.63	48.98
A	110	0.04	23.61	25.49	7.77	NA
A	130	0.03	16.97	21.84	3.04	66.37
25	5	9.97	13.70	NA	0.38	57.87
25	25	21.61	11.50	5.86	0.34	65.79
25	40	10.01	21.37	9.00	1.17	13.59
25	50	3.83	53.41	NA	6.46	20.00
25	60	0.15	19.22	NA	13.53	19.23

Figure legends

Figure 1. Map of the Mediterranean Sea with locations of sampling sites during the BOUM cruise transect. Numbered and lettered stations denote locations where our experiments were conducted.

Figure 2. Phosphate turnover time (h) of the bulk community ($> 0.2 \mu\text{m}$) over the BOUM cruise transect.

Figure 3. Abundances of *Synechococcus* (Syn), *Prochlorococcus* (Proc), picophytoeukaryotes (Pic), heterotrophic prokaryotes (Hprok) at the depths of sorted experiments at stations 9, 21, A and 25.

Figure 4. Cumulated contributions of picoplankton groups (superimposed bars for: *Synechococcus* Syn, *Prochlorococcus* Proc, picophytoeukaryotes Pic, heterotrophic prokaryotes Hprok, superimposed histograms) to the bulk P_i uptake (upper scale, 100% = measured bulk P_i uptake rate) and bulk P_i uptake rates (lower scale, white triangles) along the euphotic water column at stations 9, 21, A and 25. Dotted horizontal lines mark the deep chlorophyll maximum depth. Beware of the different vertical scales. Missing groups are specified with a *.

Figure 5. Bulk and taxon-specific P_i uptake rates (V) at increasing P_i concentrations (in situ + added) in sorted *Synechococcus* (Syn), *Prochlorococcus* (Proc), picophytoeukaryotes (Pic) and heterotrophic prokaryotes (Hprok) at St A and St. C. Straight horizontal and vertical lines represent computed V^{\max} and $K+S_n$, respectively. If a significant correlation ($p < 0.05$) between measured Pi uptake rates and those calculated from the Michaelis-Menten model, the uptake curve was fitted to the data.

Figure S1. Contribution of size fractions to total Pi uptake as a function of bulk Pi turnover time at various depths and stations along the BOUM transect.

Figure S2. Bulk Pi uptake rates (h^{-1}) plotted against SRP concentrations.

Fig. 1

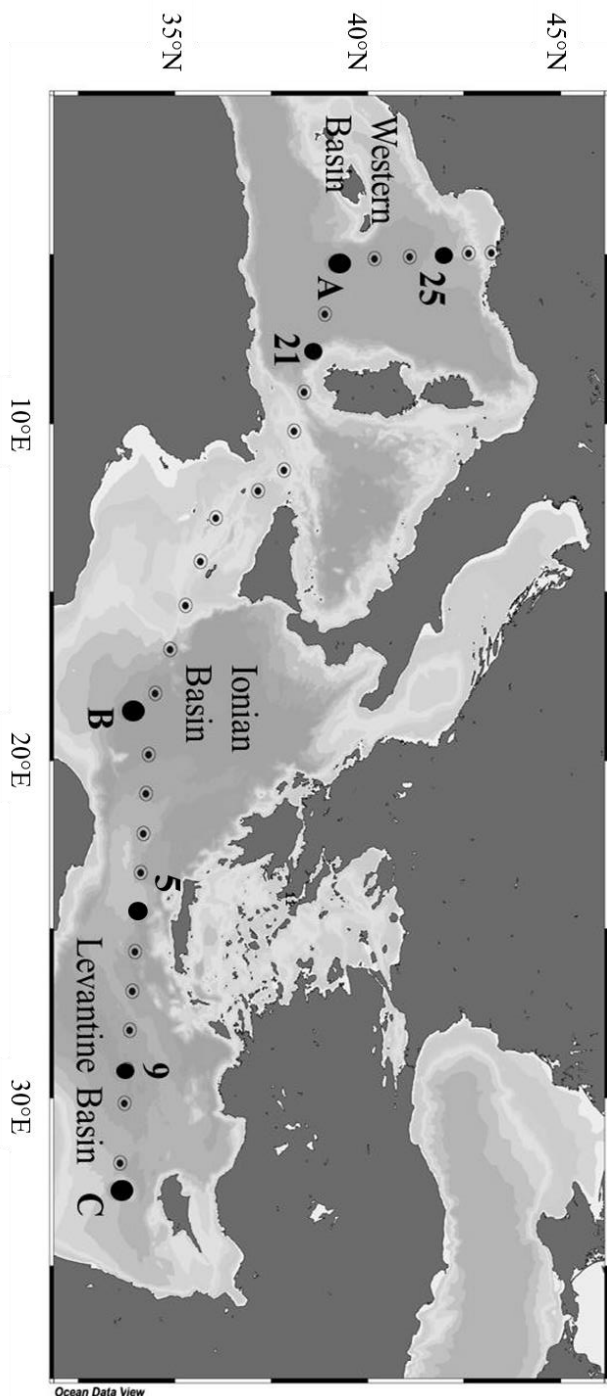


Fig. 2

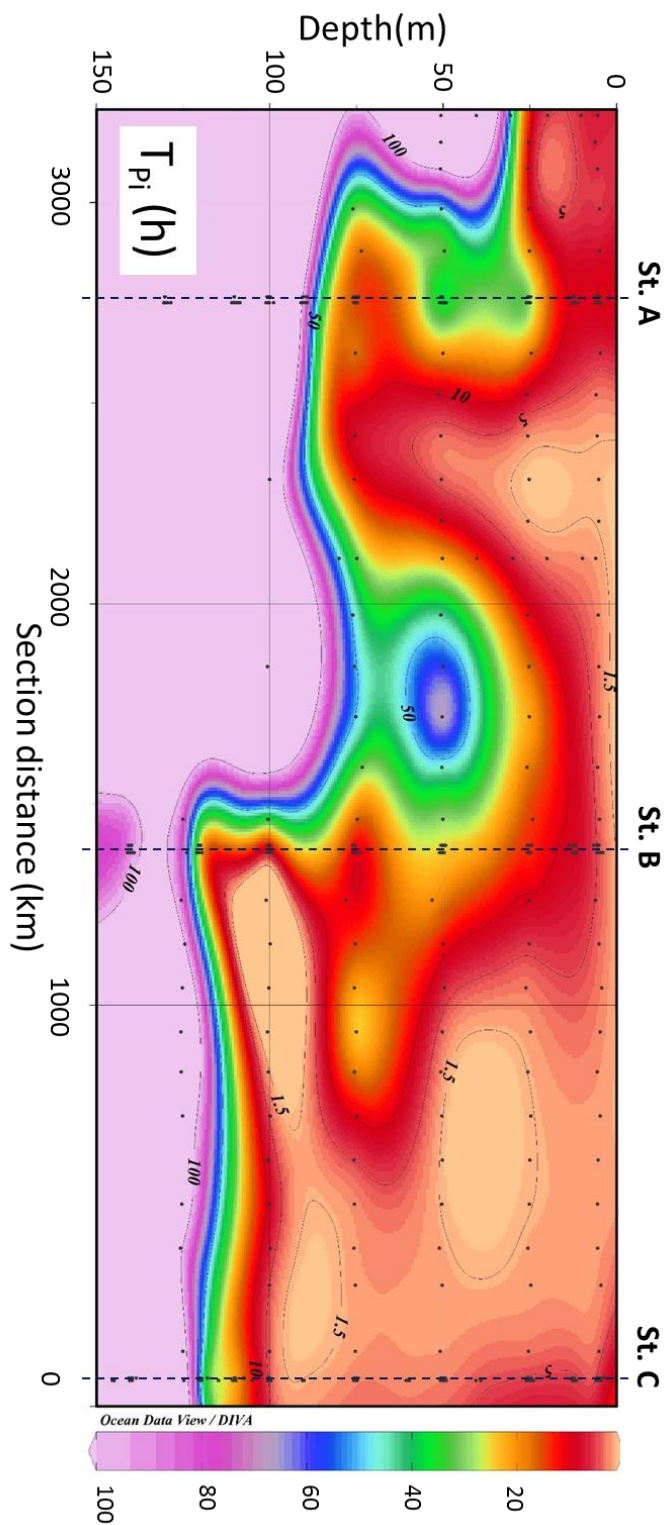


Fig. 3

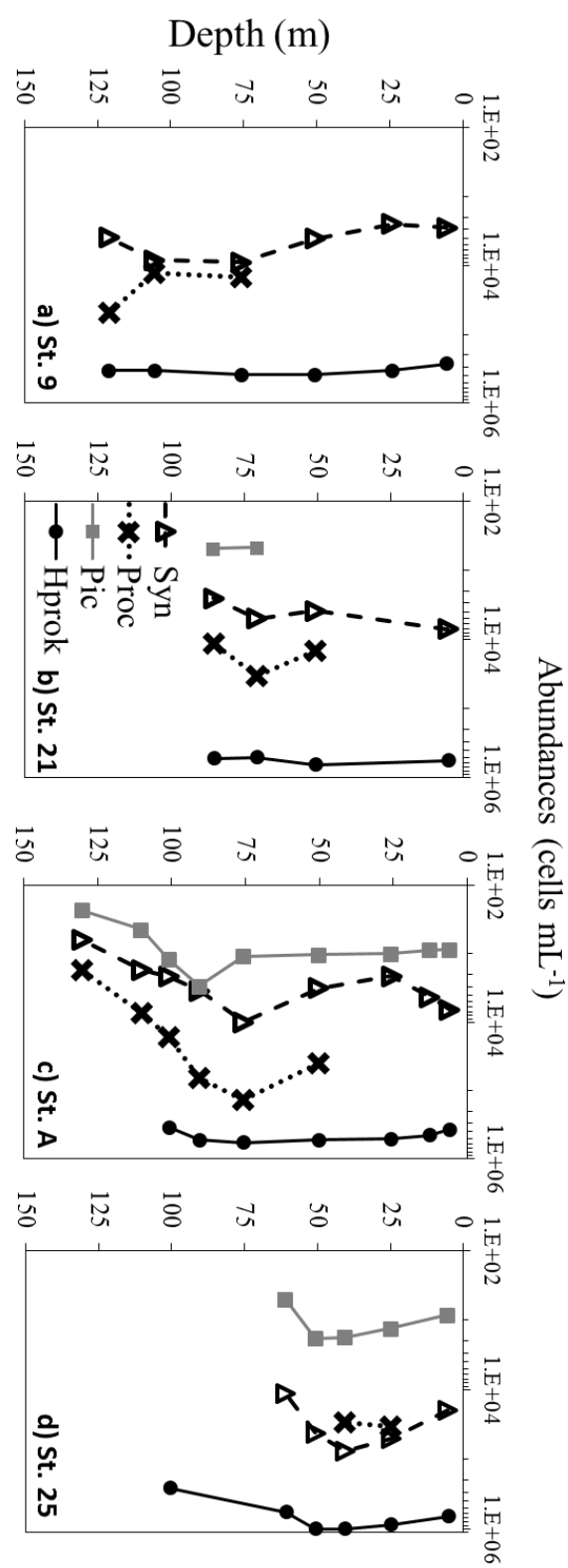


Fig. 4

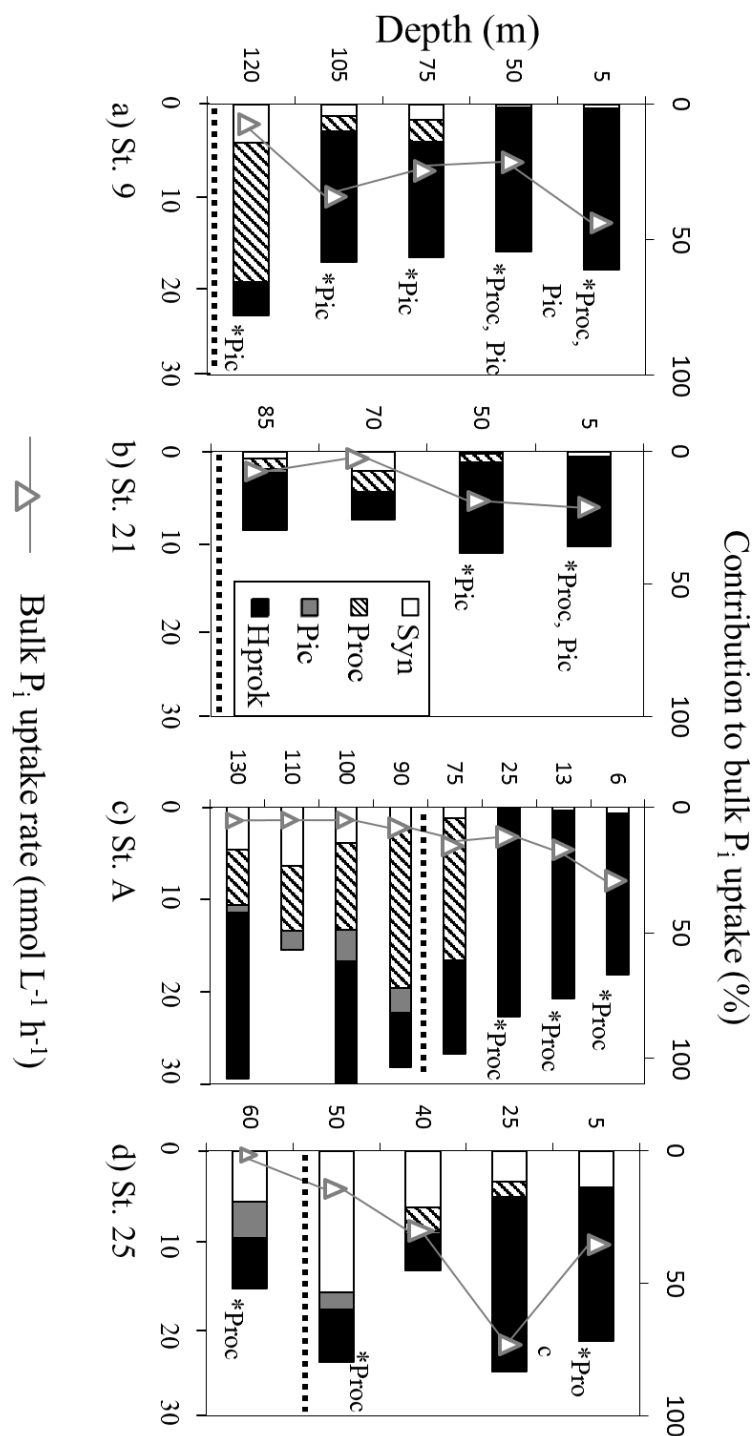


Fig. 5

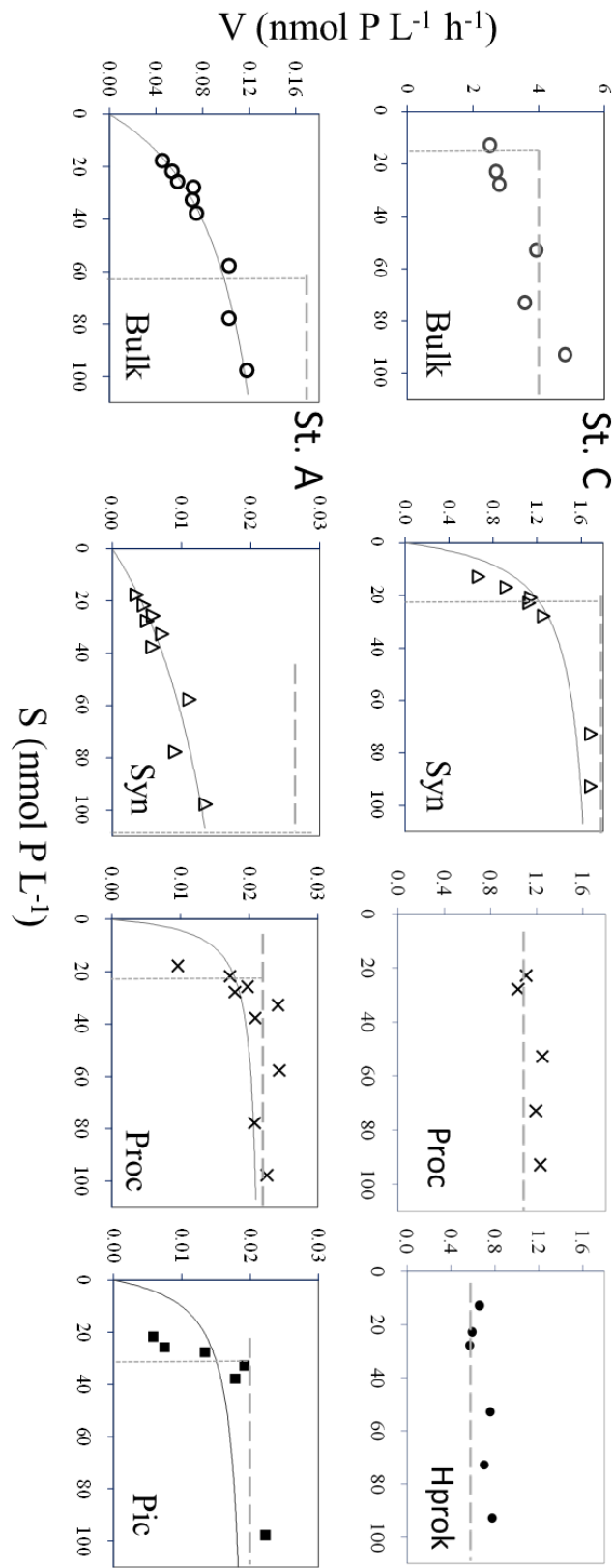


Fig. S1

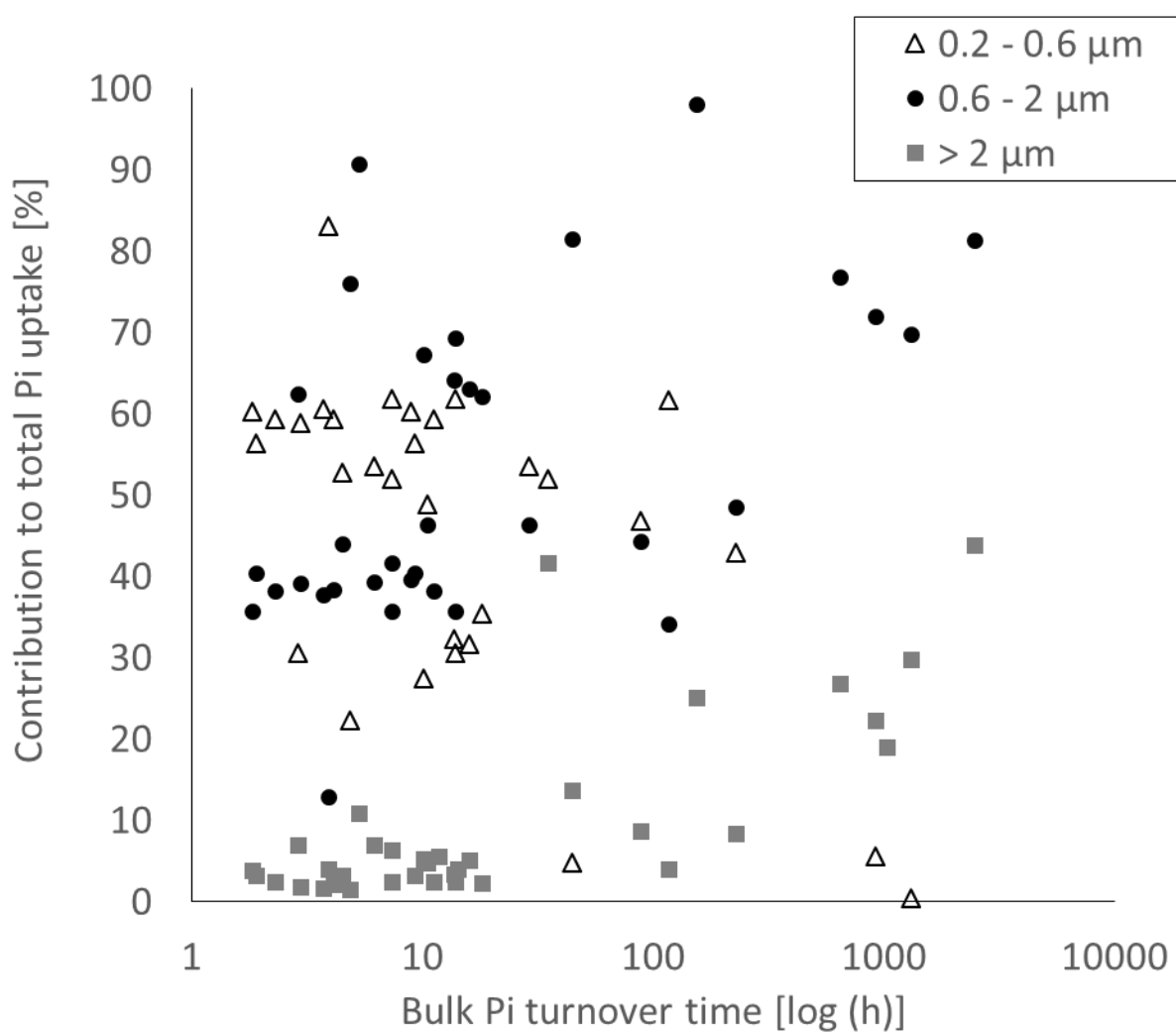


Fig. S2

